ON THE OPTIMIZATION AND PERFORMANCES OF A COMPACT PIEZOELECTRIC IMPACT MEMS ENERGY HARVESTER

Pattanaphong Janphuang, Robert Lockhart, Danick Briand, and Nico F. de Rooij
École Polytechnique Fédérale de Lausanne (EPFL), Institute of Microengineering (IMT)
The Sensors, Actuators and Microsystems Laboratory (SAMLAB), Neuchâtel, Switzerland

ABSTRACT

This paper presents the development of a compact energy harvesting configuration to convert low frequency, mechanical oscillations into usable electrical energy using AFM-like MEMS piezoelectric cantilevers coupled to a rotating gear. In this approach, one or several piezoelectric harvesters can be positioned above a rotating gear driven by an oscillating mass. In order to analyze the motion and the electrical power output from the harvester, analytical and finite element models have been developed. The harvester, with an active device volume of 3.5 mm^3 (3×5×0.23 mm^3), is able to produce an average output power of 12 μW measured across an optimal resistive load of 4.7 kΩ at a rotational speed of 19 rps, demonstrating the potential of the compact MEMS piezoelectric micro-power generator.

INTRODUCTION

Piezoelectric harvesters offer a promising solution for powering portable and implantable systems using ambient vibrations due to the ease of direct conversion from vibrational to electrical energy, achieving high power densities and straight-forward integration which is quite attractive for volume-limited applications. Piezoelectric harvesters are often implemented as inertial devices set to oscillate at their resonant frequencies; however, the typical vibration frequencies of large body movements are on the order of a few Hz (< 30 Hz) and can vary considerably over time. Thus, resonant type devices do not present a practical option. To operate resonant devices at such low frequencies, macro structures with bulky proof masses are required limiting their use for many applications.

A more promising solution for converting low frequency vibrations into usable electrical energy is impact-based energy harvesting, in which environmental motion is coupled to an inertial object through physical impacts. In recent years, impact based energy harvesting has received significant interest. Several configurations used to couple low frequency vibrations into piezoelectric transducers have been proposed and demonstrated [1]-[4]. Frequency up-conversion based on knocking or plucking has received considerable attention due to the improvement of the electromechanical coupling and efficiency of energy harvester at higher frequencies [2]. Using this mechanism, the piezoelectric harvester is struck or plucked by an inertial object exited at low frequency. The cantilever is then released to freely oscillate at its higher resonant frequency.

We previously presented a novel approach using an AFM-like MEMS piezoelectric cantilever to extract the energy from a rotating gear [4]. However, the presented configuration of the harvester assembly was bulky. Here, we present a truly compact design in which an AFM-like MEMS piezoelectric cantilever is placed directly above a rotating crown gear in order to keep the system as compact as possible. The tip of the cantilever is plucked by the vertical teeth as the gear rotates. Using the sloped vertical profile of the crown gear diminishes the amplitude of the force creating torsion in the beam. An analytical model has been developed to analyze the motion and the electrical power output from the harvester. The voltage generated is calculated by determining the stress on the deflected harvester in accordance with the motion of the gear. A more detailed description of the electromechanical behavior was studied through FEM simulations in ANSYS. Through modeling, simulation and experimental validation, we demonstrate that by modifying the gear tooth profile and the rotational speed of the gear, the performance of the harvester is significantly improved. In addition, the efficiency and longevity of the system are investigated.

CONCEPT AND MODELING

The configuration studied in this work is illustrated in Figure 1(a). A piezoelectric cantilever is placed directly above the rotating gear such that the tip at the end of the cantilever extends down between the vertically mounted gear teeth and is plucked as each tooth passes while the gear rotates in-plane.

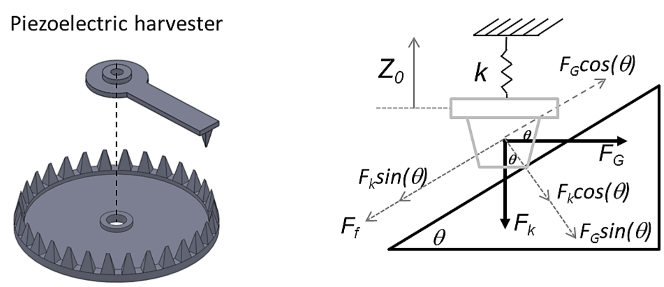

(a) (b)

Figure 1: Schematic of (a) the proposed concept (b) the plucking action between the tip and the gear tooth.

Figure 1(b) illustrates the plucking mechanism. When a gear tooth comes in contact with the tip of the cantilever, the cantilever is deflected to a certain displacement (Z_0) following the angle (θ) of the sidewall of the gear tooth profile. The angles of the sidewalls of the cantilever tip and the gear tooth also direct the force in the vertical direction while reducing the wasted force directed along the horizontal direction which is lost or used to create torsional movement of the cantilever. The interactive force between the tip and the gear tooth is represented as F_G. According to its mechanical stiffness (k), a static force applied to the tip (F_k) is created. The frictional force (F_f) from the contact surfaces acts opposite to the direction of movement. The top of the gear tooth is the release point; the cantilever falls and is free to oscillate at its resonant frequency. The mechanical work done by the gear tooth is then given by

$$W_I = \int_0^{Z_0 Sin\theta} F_G x dx = \frac{kZ_0^2}{2\tan\theta}\left(\frac{\sin\theta + \mu_k \cos\theta}{\cos\theta - \mu_k \sin\theta}\right) \quad (1)$$

where μ_k is the coefficient of friction.

Analytical modeling

A unimorph piezoelectric cantilever in this work was structured by bonding a piezoelectric layer (PZT) to a support layer (Si) of the same length (L) and width (W). For simplification, the bonding layer is ignored. The bonding between the two layers is assumed to be ideal. The polarization direction of the piezoelectric layer is through the film thickness and perpendicular to the plane (d_{31}). The cross-section of the unimorph cantilever is shown in Figure 2. t_p and t_s are the thickness of the PZT and Si, respectively.

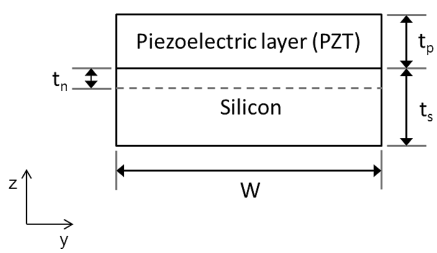

Figure 2: Cross-sectional view of the unimorph cantilever.

The lateral stress in the piezoelectric layer at a position (x, z) is given by [5]

$$\sigma = \frac{kZ_0 E_p}{(EI)_{composite}}(L-x)(z-t_n), \quad \text{for} \quad 0 < x < L \quad (2)$$

where E_p is the Young's modulus of the piezoelectric, $EI_{composite}$ is the effective bending modulus of the composite beam, and the position of the neutral plane will be at distance t_n from the interface between PZT and silicon depending on the thickness and Young's modulus of each layer. The electric field E in the PZT layer at a position (x, z) is determined by

$$E(x,z) = \frac{d_{31}}{\varepsilon}\sigma = \frac{d_{31}kZ_0E_p}{\varepsilon(EI)_{composite}}(L-x)(z-t_n) \quad (3)$$

The induced voltage generated from the PZT at x with respect to the thickness of PZT layer can be given as

$$V(x) = \int_0^{t_p} E(x,z)dz = \frac{d_{31}kZ_0E_p}{\varepsilon(EI)_{composite}}(L-x)\left(\frac{t_p^2}{2} - t_n t_p\right) \quad (4)$$

where d_{31} is the piezoelectric strain coefficient and ε is dielectric constant of piezoelectric layer. The average voltage over the length L of the harvester can be define as

$$V_{ave} = \frac{1}{L}\int_0^L V(x)dx = \frac{d_{31}kZ_0E_pL}{2\varepsilon(EI)_{composite}}\left(\frac{t_p^2}{2} - t_n t_p\right) \quad (5)$$

Deflection of the harvester as a function of the gear speed and gear tooth profile can be determined using the simple mass-spring system illustrated in Figure. 3 [6]. The force *f(t)* from the gear tooth acts on a mass *m* (representing the cantilever) which is suspended by a spring constant with a stiffness *k* and a damping element *c* resulting in the displacement *z(t)*. The second order differential equation describing the motion of the cantilever can be written as

$$m\ddot{z} + c\dot{z} + kz = F \quad (6)$$

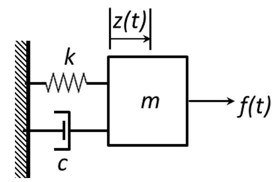

Figure 3: A generic model of impact (direct-force) generator.

In order to solve the differential equation for the dynamic displacement of the cantilever and therefore determine the output voltage from the harvester as a function of time, a fourth-order Runge-Kutta numerical model was developed in MATLAB.

FEM modeling

A transient 3D model was also developed in ANSYS 12.0 to investigate the electromechanical behavior of the designed harvester. The model predicts the voltage generated and the electrical energy produced by the harvester through a resistive load for a given input force. The analysis was based on SOLID5 (piezoelectric elements) and SOLID45 (structural elements) which include the adhesive and the silicon substrate. Using CIRCU94 elements, a resistive load (R) connects the top and bottom electrodes of the PZT layer. The boundary conditions consist of a displacement constraint on the clamped end of the cantilever. The bottom electrode of the PZT was set to ground while the top electrode was kept as a floating electrode.

The electromechanical behavior of the harvester and the plucking action between the tip and gear tooth was simulated in a transient analysis with the effects of viscous damping as illustrated in [2]. In the first step, a load is applied in which the cantilever is deflected to a certain displacement at a desired speed corresponding to the applied force. This was obtained using a ramped load solution in the model. The subsequent step is the release stage. This was simulated by removing the force from the tip of deflected cantilever allowing the cantilever to freely oscillate at its resonant frequency at the second stage of the transient analysis. The solution was simulated over several milliseconds in order to investigate the response of the harvester until the amplitude of vibration was diminished by damping. According to the simulation, the length and width of the harvester were first designed to be 5 mm and 3 mm allowing enough area to collect the generated charge while keeping a compact design. The thickness ratio of the PZT and silicon layers was designed to be close to 0.6 in order to maximize the output energy. Here, the thickness of PZT and silicon were 80 µm and 150 µm, respectively, as a compromise between flexibility and structural strength. Figure 4 gives an example of the simulated open circuit voltage (at 1 MΩ) from the designed harvester at different rotational speeds.

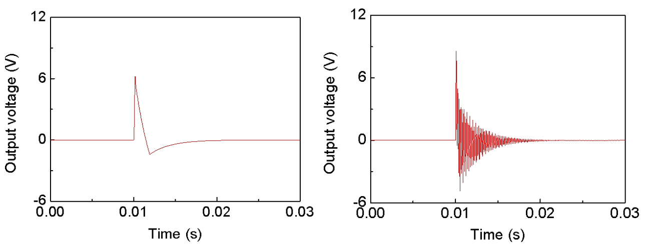

(a) (b)

Figure 4: Simulated output voltage across resistive load of 1 MΩ as a function of time at the rotational speed of (a) 3 rps (b) 19 rps.

The average power and energy produced at the time t_N can be calculated using the following expression

$$P(t_N) = \frac{1}{t_N}\int_0^{t_N} \frac{V^2(t)}{R} dt \tag{7}$$

$$E(t_N) = \sum_{i=0}^{N} P(t_i)\Delta t_i , \qquad \text{for N > 0} \tag{8}$$

Where t_i is the time at sub-step i.

RESULTS AND DISCUSSION

Piezoelectric harvesters were fabricated by bonding an 80 µm-thick PZT-5A layer onto a micromachined silicon AFM-like cantilever. More details about the fabrication process and experimental setup are illustrated in [4].

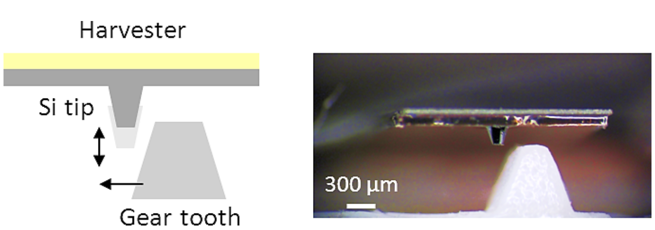

Figure 5: The harvester mounted on the X, Y and Z stage and positioned above the gear.

The power generation of the impact-type piezoelectric harvesters was observed by varying the tip insertion depth into a crown gear and adjusting the rotational speed of the gear as shown in Figure 5. Figure 6 presents an example of the generated voltage and energy transferred from a harvester to an optimal load resistance. Post-excitation oscillations of the harvester were not observed at slow rotational speeds (<3 rps) - the tip of the cantilever simply follows the contour of the gear tooth as predicted by simulations (Figure 6(a)). Free oscillations of the harvester after plucking, however, are clearly observed for rotational speeds at 19 rps (Figure 6(b)).

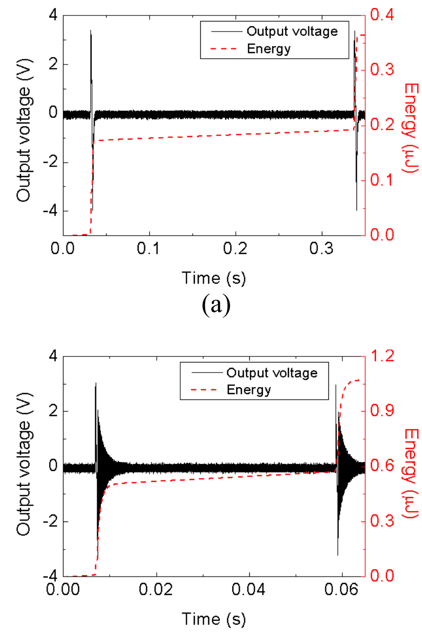

(a)

(b)

Figure 6: (a) Output voltage and energy dissipated in the optimal resistor at rotational speed of (a) 3 rps. (b) 19 rps.

At rotational speeds of 3 rps, most of the energy is produced during the deflection of the cantilever. For one cycle, the energy was found to reach a maximum of 0.2 µJ at an optimal load of 119 kΩ. At higher rotational speeds (19 rps) (Figure 5(b)), the harvester was capable to producing an energy of up to 0.6 µJ at 4.7 kΩ.

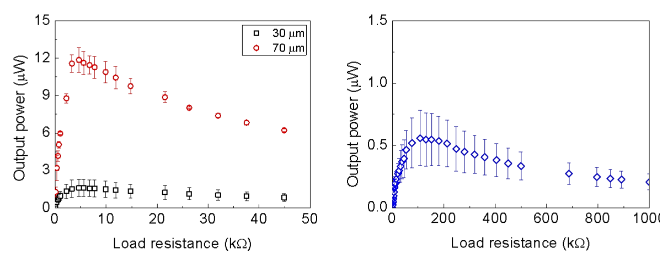

(a) (b)

Figure 7: (a) Output power as a function of tip depth at rotational speed of 19 rps. (b) Output power at rotational speed of 3 rps and 70 µm tip depth.

The energy produced in the release step is significant. More than 80 % of the energy was produced during the free oscillations. The optimal load resistance (R_{opt}) can be approximated using $R_{opt} = 1/\omega C_p$ where ω is the natural frequency of the harvester and C_p is the capacitance of the piezoelectric layer. As the rotational speed dropped to 3 rps, the optimal load resistance increased to 119 kΩ due to a lack of oscillations after plucking. As a result, ω, which is a combination of the plucking frequency and the resonant frequency of the harvester [3], dropped causing the optimal load to increase.

Figure 7(a) presents the output power as a function of tip depth. At a rotational speed of 19 rps, the harvesters can generate an average output power of 12 μW (over one cycle) at a tip depth of 70 μm. As the rotational speed dropped to 3 rps, the output power also dropped to 0.6 μW due to limited oscillations of the harvester as describe above and to the fact that the time integral of the average power was increased as a result of the longer plucking period (Figure 7(b)). The results of the analytical calculation and the FEM simulations show good agreement with the experimental measurement as shown in Figure 8.

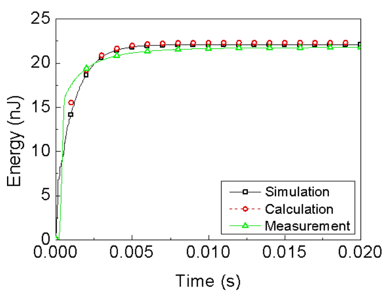

Figure 8: Comparison between simulation and experiment of the energy dissipated in the load resistance of 1 MΩ at rotational speed of 19 rps.

The overall efficiency of this approach was determined using a rotational flywheel as illustrated in [7]. The efficiency of the configuration was found to be 0.6 % at a tip depth of 70 μm for rotational speeds between 20 rps and 18 rps. The efficiency drops gradually as the speed is reduced.

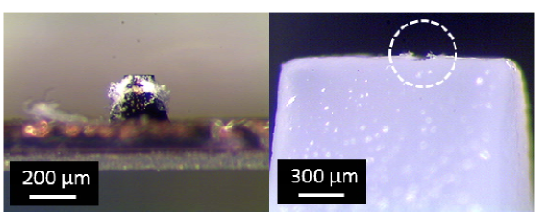

Figure 9: Optical images of the silicon tip (left) and top view of a gear tooth (right) after the lifetime test.

The reason for low efficiency was mainly due to friction from the coupling between the two structures. Finally, the reliability of this configuration was investigated by monitoring the voltage generated as a function of the number of plucks. In the experiment, a crown gear with 36 teeth coupled to an electric motor rotating at 19 rps was used in the test.

The output voltage dropped approximately 33 % after 8 million plucks. The decrease in the output voltage was mainly caused by erosion of the acetal polymer gear by the silicon tip as shown in Figure 9. This demonstrates the significance of the materials used and the geometry of the tip/tooth profile for the reliability of this approach. Materials and wearless coatings are being investigated to reduce the wear problem and improve the efficiency and longevity of this harvesting system.

CONCLUSIONS

A compact configuration for harvesting energy from low frequency movement using the impact between a rotating gear and a piezoelectric MEMS harvester has been successfully demonstrated in this paper. This concept could be combined with an oscillating mass-gear mechanism to realize a compact autonomous micro-power generator from body movements as well as other rotating objects.

REFERENCES

[1] M. Renaud, P. Fiorini, R. van Schaijk, and C. van Hoof, "Harvesting energy from the motion of human limbs: the design and analysis of an impact-based piezoelectric generator", *Smart Mater. Struct.*, vol. 18, pp. 035001-035016, 2009.

[2] M. Pozzi and M. Zhu, "Plucked piezoelectric bimorphs for knee-joint energy harvesting: modeling and experimental validation", *Smart Mater. Struct.*, vol. 20, pp. 055007-055016, 2011.

[3] L.Gu, and C. Livermore, "Impact-driven, frequency up-converting coupled vibration energy harvesting device for low frequency operation", *Smart Mater. Struct.*, vol. 20, pp. 045004-045013, 2011.

[4] P. Janphuang, D. Isarakorn, D. Briand, and N.F. de Rooij, "Energy harvesting from a rotating gear using an impact type piezoelectric MEMS scavenger," in *Digest Tech. Papers Transducers'11 Conference*, Beijing - China, June 5-9, 2011, pp. 735-738.

[5] X. Gao, W.H. Shih, and W.Y. Shih, "Induced voltage of piezoelectric unimorph cantilevers of different nonpiezoelectric/piezoelectric length ratios", *Smart Mater. Struct.*, vol. 18, pp. 125018-125025, 20091.

[6] P.D. Mitcheson, E.M. Yeatman, G. Kondala Rao, A.S. Holmes, and T.C. Green, "Energy harvesting from human and machine motion for wireless electronic devices", *Proceedings of the IEEE*, vol. 96, pp. 1457-1486, 2008.

[7] P. Janphuang, R. Lockhart, S. Henein, D. Briand, and N.F. de Rooij, "On the experimental determination of the efficiency of piezoelectric impact-type energy harvesters using a rotational flywheel," *Tech paper PowerMEMS Conference*, London - UK, December 3-6, 2013.

CONTACT

*P. Janphuang, tel: +41-(0)2-6954435;
pattanaphong.janphuang@epfl.ch